Understanding Excess Pore Water Dissipation in Soil Liquefaction Mitigation

Siau Chen CHIAN[1] and Saizhao DU[2]

[1] National University of Singapore, Singapore 117576, Singapore
[2] Beijing Jiaotong University, Beijing 100044, China
sc.chian@nus.edu.sg

Abstract. Soil liquefaction has conventionally been studied in cyclic laboratory tests as a pure undrained condition, assuming that excess pore water pressure is unable to dissipate during rapid shearing. As such, dissipation of excess pore water pressure generated during shearing is often not modelled in classic cyclic simple shear and triaxial tests. In contrast, dissipation of excess pore pressure does occur in the field following major earthquakes in the form of severe ground settlement and sand boils where fine granular soils were found. In this theme lecture, two aspects of soil liquefaction are discussed. First, a study on the interaction of excess pore water pressure generation and dissipation on liquefiable clean sand in the cyclic triaxial test setup is conducted. Results show that pore water dissipation at merely a fraction of the permeability of the soil can have a significant effect to the soil's susceptibility to liquefaction. This calls for future cyclic laboratory tests to adopt similar near-perfect undrained condition to better reflect a more realistic representation of soil liquefaction in the field. Second, a critical cyclic shear stress ratio is obtained, where excess pore pressure dissipation dominates excess pore pressure generation, beyond which the soil is no longer susceptible to liquefaction. Complementing this ratio is the identification of a critical void ratio in which the excess pore pressures do not build up despite considerable shearing amplitude, implying the soil is no longer susceptible to liquefaction at that degree of densification. Such information would serve as a guidance to mitigate soil liquefaction in soil densification operations.

Keywords: Soil Liquefaction, Pore Pressure, Generation, Dissipation, Cyclic Shear Stress Ratio, Void Ratio.

1 Introduction

Damage caused by soil liquefaction following strong earthquakes persist to date as evident in recent earthquake events such as the 2016 Muisne [1], 2011 Tohoku [2], 2011 Christchurch [3], 2010 Maule [4] and 2009 Padang [5]. Earthquake induced soil liquefaction can lead to damaged relating to excessive ground settlement, lateral spreading, foundation failures and uplift of underground infrastructure. The phenomenon of soil liquefaction is caused by the buildup of excess pore water pressure when

loose saturated granular soil is subjected to rapid shearing in which the pore water is unable to escape from the collapsing voids within the soil particles. As such, permeability during the shearing is a crucial parameter to consider in the development of excess pore water pressure.

At present, single element laboratory studies on soil liquefaction using cyclic simple shear and triaxial shear testing are often limited to undrained condition. This implies that dissipation of pore water is ignored. In contrast, observations from geotechnical centrifuge modelling [6] and video footages of the ground following the 2011 Tohoku Earthquake [7] do indicate that pore pressure generation and dissipation do take place concurrently, often in the form of sand boils. The importance of pore water drainage is also inferred by most liquefaction induced failures taking place during the dissipation phase [8]. In this paper, small amount of pore water drainage in cyclic triaxial testing to mimic some dissipation of excess pore water pressure during shearing is introduced to offer a closer presentation of the field condition.

2 Cyclic Triaxial Setup with Drainage

2.1 Soil Properties

A series of cyclic triaxial testing were carried out to investigate the influence of small amount of drainage (i.e. a near perfect undrained condition) on the impact of soil liquefaction. The granular soil used in these tests was fine grained uniform silica sand with particle size distribution presented in Fig. 1. The physical geotechnical properties of the sand are presented in Table 1.

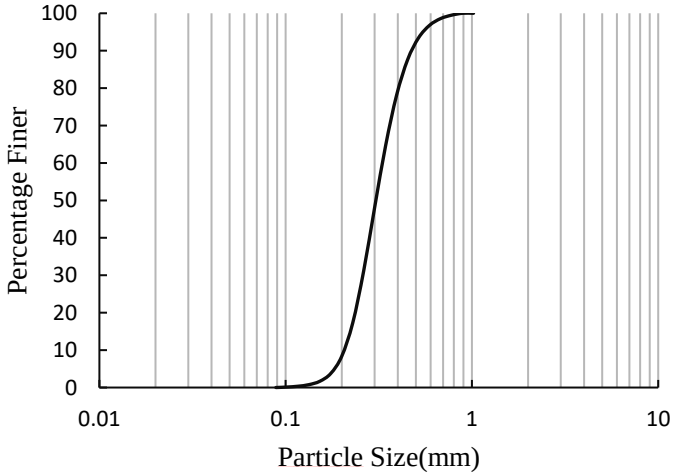

Fig 1. Particle size distribution of silica sand used

Table 1. Physical properties of silica sand

Properties	Values
Φ_{crit}	34°
G_s	2.65
e_{max}	0.86
e_{min}	0.48
D_{10}	0.22mm
D_{50}	0.26mm
D_{90}	0.48mm

2.2 Triaxial Setup

The cyclic triaxial testing was carried out on a GDS enterprise level dynamic triaxial testing system (ELDYN), based on an axially-stiff load frame with a beam mounted electro-mechanical actuator. Two sets of pressure controllers, each connecting to the ends of the cylindrical soil samples, were adopted to record the amount of water flowing into or out of the sample. This permits measurement of permeability as well as computation of void ratio changes during testing. Fig. 2 shows the setup of the modified triaxial system.

Cylindrical soil samples of 76mm and 38mm in height and diameter were prepared using air pluviation in a rubber membrane with porous stones and filter paper on each end. In order to facilitate pluviation of sand into the membrane, vacuum was applied on the outside of the membrane to keep the membrane upright. Higher densities of soil samples were achieved by raising the fall height while pouring sand into the membrane. After completion of sand pouring, the dry sand sample was saturated with de-aired water using the back pressure inlet of the triaxial setup. Thereafter, the sample was consolidated isotropically to the target final effective isotropic confining pressure. This marks the end of sample preparation and the sample ready to be sheared.

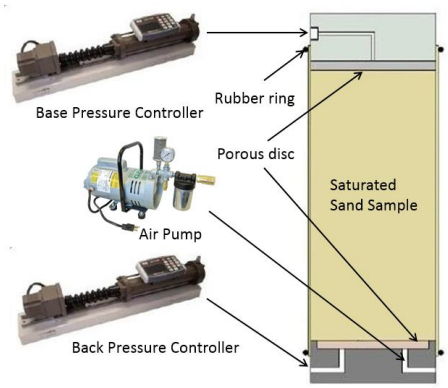

Fig. 2. Setup of modified triaxial setup

Triaxial permeability tests were carried out using the same sand and similar density and effective confining pressure. At static condition, the coefficient of permeability for a fully saturated sand sample was about 5 x 5×10^{-4}m/s (or flow rate of about 7400mm^3/s for a 38mm diameter sample) under a pressure difference of 10kPa. In order to study the impact of pore water dissipation, 3 different flowrates (5, 10 and 20mm^3/s) far lower than the static permeability of the sand to ensure a near-perfect undrained condition.

2.3 Test Programme

The cyclic triaxial tests involved shearing the sand undrained till liquefaction to maintain the height and diameter of sample, before transiting to stress-controlled shearing with allowance of little drainage outflow to take place as illustrated in Fig. 3. Soil samples were consolidated under an initial effective isotropic confining stress of about 75 kPa and sheared at a frequency of 0.2 Hz. In Table 2, the tests were to investigate the dissipation profile resembling consolidation on self-weight and dependent on permeability of the liquefied soil (i.e. Test D-0-5) as well as study the impact of pore water expulsion from the ground (i.e. small amount of drainage) during earthquake shaking which is prevalent in the field. The permeability of the sand obtained from triaxial permeability test was 5×10^{-4}m/s or flow rate of 7400mm^3/s for a 38mm diameter sample. Hence, discharge rates in Table 2 are comparatively low.

Table 2. Details of cyclic triaxial tests conducted

Amplitude (kN)	σ (kPa)	Q (mm³/s)	Dissipation stage (start with $r_u \geq 0.95$)			
			Test ID	e_0	Dr,$_0$ (%)	R
0	0	5	D-0-5	0.714	38.3	0.00
0.01	8.8	5	D-0.01-5	0.698	42.6	0.06
		10	D-0.01-10	0.694	43.7	0.06
		20	D-0.01-20	0.688	45.3	0.06
0.05	44.1	5	D-0.05-5	0.692	44.2	0.30
		10	D-0.05-10	0.696	43.2	0.30
		20	D-0.05-20	0.700	42.1	0.30
0.1	88.2	5	D-0.1-5	0.710	39.5	0.59
		10	D-0.1-10	0.702	41.6	0.59
		20	D-0.1-20	0.697	42.9	0.59
0.15	132.3	5	D-0.15-5	0.714	38.4	0.88
		10	D-0.15-10	0.708	40.1	0.88
		20	D-0.15-20	0.705	40.8	0.88

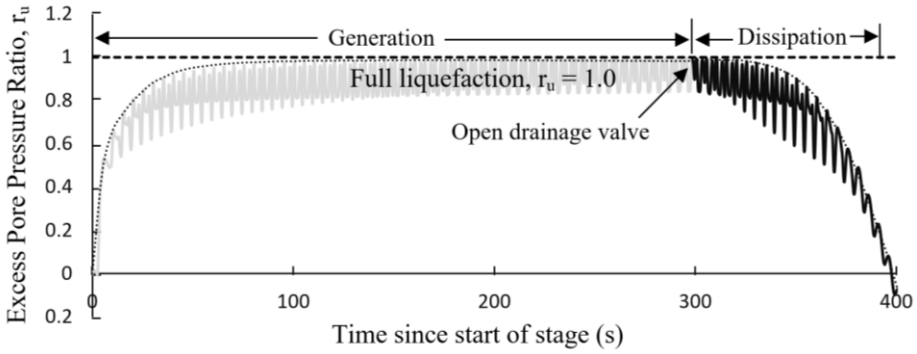

Fig. 3. Cyclic triaxial test with generation and dissipation

3 Results and Discussion

3.1 Effect of Discharge on Excess Pore Pressure Dissipation

Based on Table 2, for the test involving no shearing during dissipation (Test D-0-5), a parabola behaviour in excess pore pressure dissipation was observed as expected in Fig. 4a. In the case of continual shearing during dissipation, full liquefaction was maintained for few loading cycles before excess pore pressure ratio commenced its decline as demonstrated in Fig. 4b to e. This implies that prior to the decline while partial drainage was permitted, the rate of excess pore pressure generation was larger than dissipation during those few loading cycles. However, over time, the allowance of drainage would lead to the reduction in volume of the soil sample by means of collapsing of large voids. Eventually, the soil sample would possess a greater resistance to liquefaction due to densification which is demonstrated with the increasing rate of decline in excess pore pressure ratio observed. It can also be observed that a larger cyclic stress amplitude would prolong the full liquefaction regime since larger stress amplitudes are expected to generate greater excess pore pressure generation. Such greater excess pore pressure generation is also supported by the gentler slope of the excess pore pressure decline for larger stress amplitude tests.

Fig. 5 shows the effect of discharge flowrate on the dissipation of excess pore water pressure. It can be observed that the discharge flowrate has a similar but opposite effect as compared to the cyclic stress amplitude. A larger discharge flowrate lead to a more rapid rate and commencement of excess pore pressure reduction. This is despite the flowrate being excessively low as compared to the static permeability of the soil, which infers that the assumption of undrained condition of earthquake induced soil liquefaction may lead to overdesign of infrastructure due to prolong effects of soil liquefaction in the simulation.

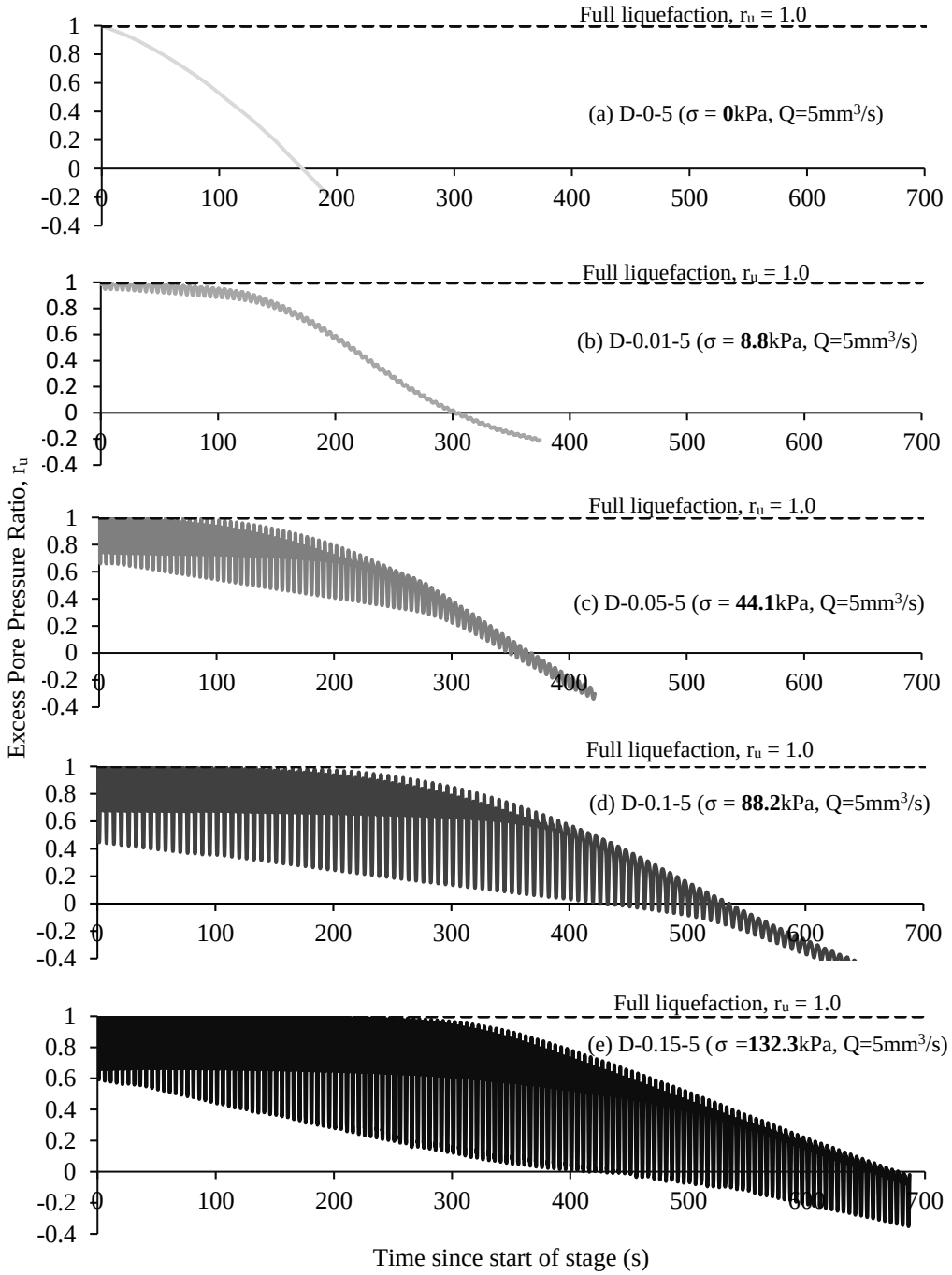

Fig. 4. Post liquefaction dissipation at different cyclic shear stress amplitude σ

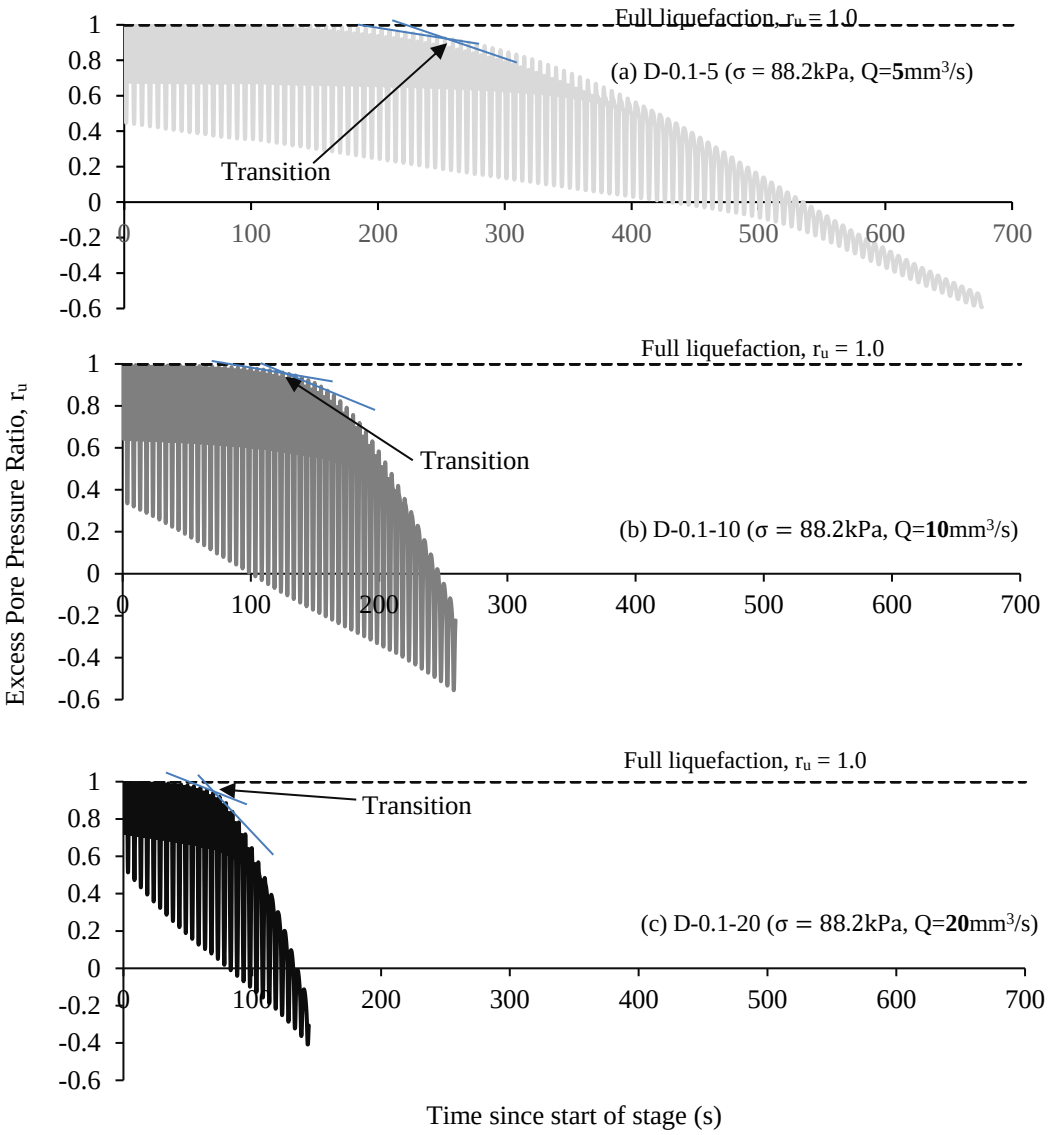

Fig. 5. Post liquefaction dissipation at different discharge flowrate Q

In order to make comparison between tests, the juncture of transition from an excess pore water pressure generation to excess pore water pressure dissipation dominant behaviour is identified as the point in time where maximum pore pressure change per

unit cycle (i.e. the point of steepest slope of $\frac{\Delta u}{t}$) is observed from a near linear trend (see Fig. 5). Fig. 6 shows the relationship between shear stress amplitude, flowrate and volumetric strain. These data points refer to the volumetric strains where excess pore pressure profiles began to fall under coupled shear loading and draining (i.e. transition point). It is interesting to note that these points show a sharp rise in shear stress amplitude at the juncture of about 0.02% volumetric strain. This persists even at different flowrate, thereby demonstrating similar limiting packing of the sand grains where liquefaction susceptibility is reduced dramatically.

Since a limiting condition exists with respect to the packing of sand grain, a detailed analysis with the use of void ratio is conducted to ascertain the significance of the limit volumetric strain observed. Their excess pore pressure dissipation and void ratios are presented in Fig. 7. The figure shows that the void ratios which marks the commencement of decline of excess pore pressure (i.e. at transition point) were similar in magnitude at 0.688 for these tests, despite differing initial void ratios and stress amplitudes. This indicate the critical void ratio to be about 0.688 where excess pore pressure generation can no longer surpass the dissipation to support the high excess pore pressure in the sand.

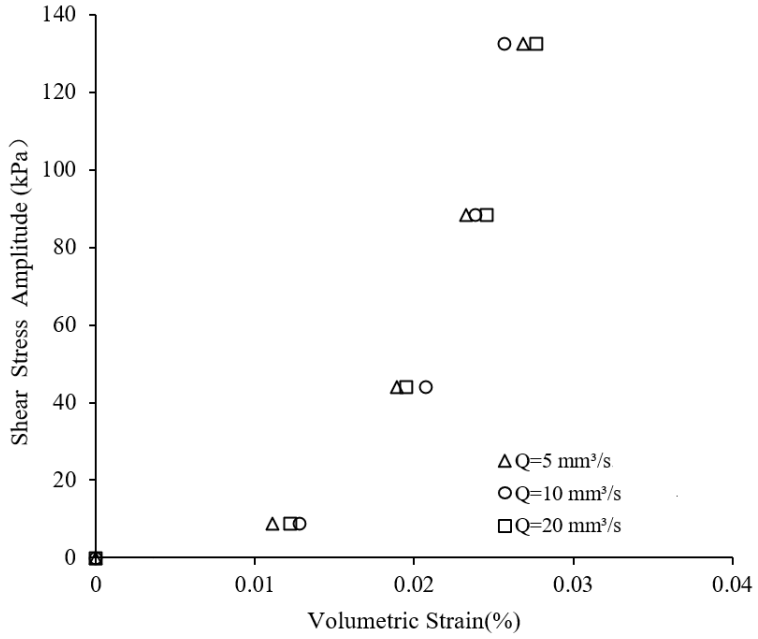

Fig. 6. Cyclic shear stress amplitude versus volumetric strain at transition with different discharge flowrate

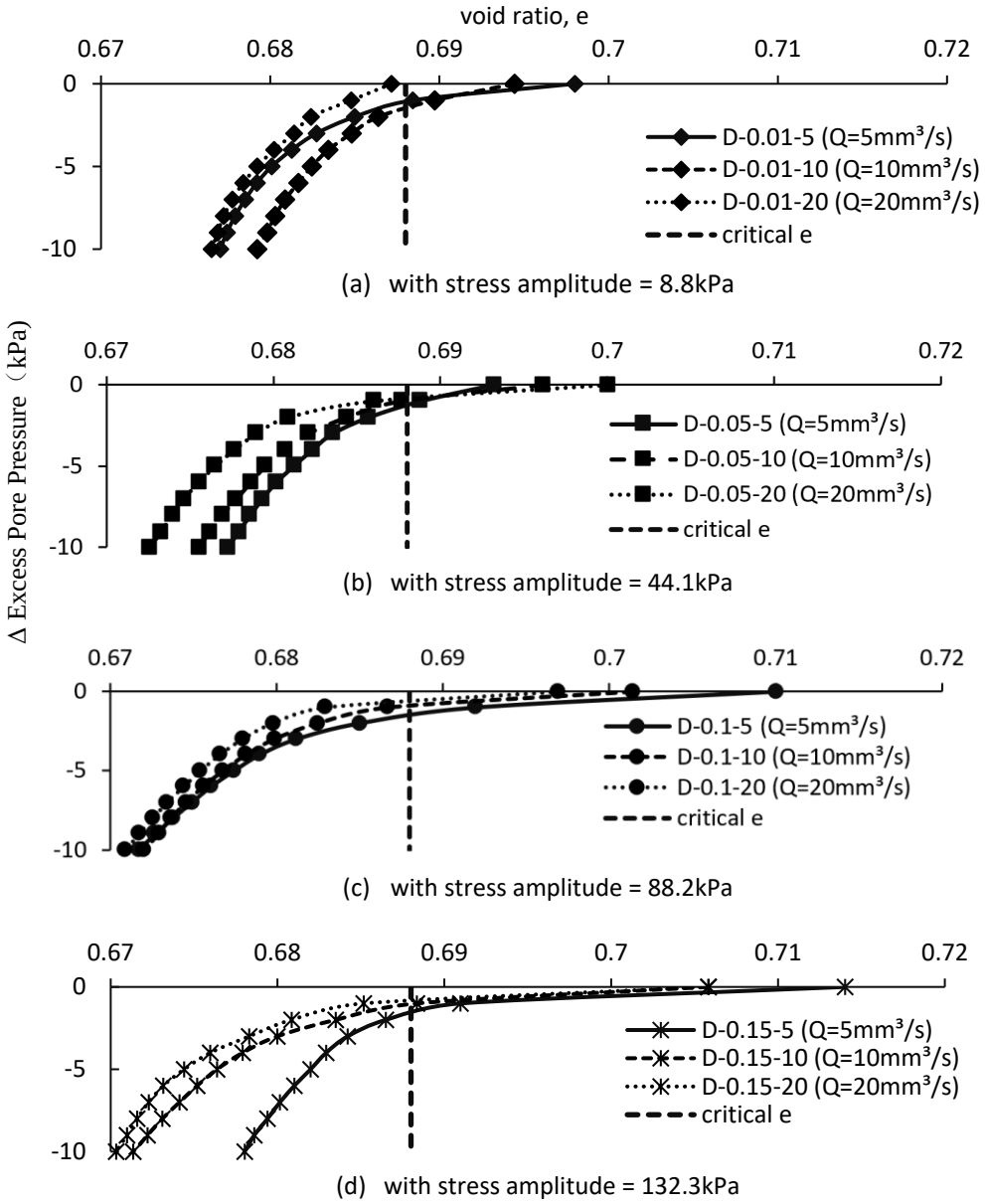

Fig. 7. Critical void ratio on pore pressure dissipation with different stress amplitude.

The minimum degree of densification is influenced by both arrangement of sand grain and cyclic shear stress ratio. As shown in Fig. 5, higher flowrate requires less time to dissipate the entire excess pore pressure and vice versa. The outcome results in consistent amount of water flowed out of sample, i.e. consistent reduction in void ratio e at similar volumetric strain, suggesting that minimum degree of densification exists under similar cyclic shear stress amplitude and confining pressure condition. Determining such critical void ratio may well provide guides on the minimum degree of densification of the sand as part of conventional soil liquefaction mitigation measures.

References

1. Franco G., Stone H., Ahmed B., Chian S.C., Hughes F., Jirouskova N., Kaminski S., Lopez J., van Drunen N.G. and Querembas M.: The April 16 2016 Mw7.8 Muisne earthquake in Ecuador – Preliminary Observations from the EEFIT reconnaissance mission of May 24 – June 7. In: *16th World Conference on Earthquake Engineering*, Paper No. 4982. (2017).
2. Chian S.C., Tokimatsu K. and Madabhushi S.P.G.: Soil liquefaction-induced uplift of underground structures: Physical and numerical modeling. *Journal of Geotechnical and Geoenvironmental Engineering*, ASCE, 140(10), 04014057. (2014).
3. Earthquake Engineering Research Institute (EERI): The M 6.3 Christchurch, New Zealand. Earthquake of EERI February 22, *EERI Special Earthquake Report.* (2011).
4. Geoengineering Extreme Events Reconnaissance (GEER): Geo-engineering reconnissance of the 2010 Maule, Chile earthquake, *Report of the NSF Sponsored GEER Association Team*. (2010).
5. Wilkinson S.M., Alarcon J.E., Whittle J. and Chian S.C.: Observations of damage to building from Mw 7.6 Padang earthquake of 30 September 2009. Natural Hazards, 63: 521-547. (2012).
6. Chian S.C. and Madabhushi S.P.G.: Influence of fluid viscosity on the response of buried structures under earthquake induced liquefaction. *7th International Conference on Physical Modelling in Geotechnics.* Zurich, pp. 111-115. (2010).
7. Goldberg S.: See the ground actually open up and move. YouTube website, https://www.youtube.com/watch?v=TzlodnjPAuc, last accessed 2021/12/30.
8. Kramer S.L.: Geotechnical Earthquake Engineering. Prentice Hall. New York. (1996).